Scripta Materialia 113 (2016) 250–253

Contents lists available at ScienceDirect

Scripta Materialia

journal homepage: www.elsevier.com/locate/scriptamat

Regular Article

Strength of hierarchically porous ceramics: Discrete simulations on X-ray nanotomography images

Denis Roussel [a], Aaron Lichtner [b], David Jauffrès [a], Julie Villanova [c], Rajendra K. Bordia [d], Christophe L. Martin [a,*]

[a] Univ. Grenoble Alpes, CNRS, SIMAP, F-38000 Grenoble, France
[b] Department of Materials Science and Engineering, University of Washington, Roberts Hall, Box 352120, Seattle, WA 98195, United States
[c] ESRF The European Synchrotron, CS 40220, 38043 Grenoble Cedex 9, France
[d] Department of Materials Science and Engineering, Clemson University, 161 Sirrine Hall, Clemson, SC 29634-0971, United States

ARTICLE INFO

Article history:
Received 19 October 2015
Received in revised form 3 November 2015
Accepted 11 November 2015
Available online xxxx

Keywords:
Porous material
Fracture
Three-dimensional tomography
Discrete simulations

ABSTRACT

Porous ceramic samples were processed either by freeze-casting or by slip-casting with pore formers. They were partially sintered to obtain a total porosity in between 44 and 69%. Samples were imaged by X-ray nanotomography with 75 nm resolution. The images, approximately 70^3 to 90^3 μm^3 in size, were merged with randomly packed particles to obtain representative numerical microstructures. The numerical samples were crushed uniaxially using discrete element simulations with appropriate microscopic fracture properties. This revealed anisotropic behavior for freeze-cast samples. Simulated strength values were compared to experimental data, with some consideration given to sample volume.

Among the various applications requiring highly porous ceramics, filters, scaffolds for bone generation, and the electrodes in solid oxide fuel cells (SOFC) are of great engineering relevance. The functional properties of interest for these applications (permeability, bioactivity, chemical reactivity and electrical and/or thermal conductivity) are mainly dictated by the amount and morphology of their porosity. The microstructural requirements needed for optimal levels of these functional properties often contradict with the need for some required mechanical performance, especially in regard to strength [1,2]. Indeed, inherent brittleness and flaw sensitivity severely limit the potential use of porous ceramics. Thus, accurate methods relating strength and microstructure are needed for this important class of materials.

X-ray tomography and focused ion beam/scanning electron microscope (FIB/SEM) tomography offer the ability to reconstruct in 3D, a representative material volume that can capture important properties. If this volume is sufficiently large, properties such as contiguity, tortuosity [3], thermal conductivity [4], elasticity [5,6] and elastic limit [7] can be calculated. This is typically carried out by meshing the images using standard Finite Element Methods (FEM). However, starting from tomography images, fracture is a more elusive property to simulate. This is because fracture involves local topological modifications (branching, bifurcation, healing and new surface generation) that are difficult to capture even with cohesive zone models [8]. With this in mind, we show how the Discrete Element Method (DEM) can be coupled with X-ray nanotomography images of porous ceramics to compute their strength and elucidate their fracture mechanisms.

Porous ceramics for SOFC cathode application were processed using an aqueous composite ceramic slurry composed of a 60:40 volume ratio of yttria-stabilized zirconia (YSZ, ion-conducting) and lanthanum strontium manganite (LSM, electron-conducting) powders. The slurry is obtained by mixing ceramic particles (d_{YSZ} = 300 nm and d_{LSM} = 800 nm) into an aqueous solution containing an organic dispersant (Darvan C-N) and a binder (PEG) [9,10]. Two types of microstructures were processed. Directional freeze-casting was used to create anisotropic samples. In this case, the slurry was poured into a cylindrical mold and cooled from one side using a temperature profile of 10 °C min^{-1} until the slurry had completely solidified (see [9,10] for a detailed study of the effect of freezing rate on microstructure). Subsequent sublimation of the ice led to a porous green-body. Two values of solid loading in the initial slurry (17 and 27 vol.%) were used to produce different values of porosity after sintering. The 17 and 27 vol.% solid loadings resulted in average wall size of 15 μm and 25 μm, respectively. For the freezing rate investigated here, the macropore size (after sintering) does not depend on solid loading and is approximately 10 μm.

Isotropic microstructures were produced by adding PMMA pore formers (d_{PMMA} = 10 μm) into a slurry that was then slip-cast using cylindrical molds. The size of the pore formers was selected to match the size of macropores obtained by freeze-casting (but with a narrower size dispersion). Both types of green bodies were sintered at 1200 °C with a 2 h dwell time [10].

* Corresponding author.
E-mail address: christophe.martin@simap.grenoble-inp.fr (C.L. Martin).

http://dx.doi.org/10.1016/j.scriptamat.2015.11.015
1359-6462/

X-ray nanotomography was performed at the nano-imaging end station (ID19) of the European Synchrotron Research Facility (ESRF) to obtain 3D microstructural representations of the anisotropic and isotropic samples [11]. Four anisotropic and two isotropic samples were imaged (Fig. 1). Their total porosity levels (hereafter denoted as ε), evaluated by image analysis and confirmed by Archimedes measurements, ranged between 44% and 69%, depending on the solid loading in the slurry, 27 and 17%, respectively. For freeze-cast samples, ε is the sum of the wall porosity and of the macroporosity in between walls (see Fig. 3 in [12]). Isotropic and anisotropic samples experienced shrinkage of the order of $20 \pm 1\%$ and $17 \pm 2\%$ during sintering, respectively. Anisotropic samples (Fig. 1(a–d)) exhibit large pores (macroporosity) aligned with the freezing direction (z). The macroporosity in anisotropic samples is arranged in colonies at a larger scale. These colonies are typically 100 to 500 μm. Within these colonies, pores align with each other, leading to an additional level of architecture (Fig. 2a). All the images of anisotropic samples were taken fully within a given colony, i.e. images do not span over several colonies.

The 75 nm resolution attained by X-ray nanotomography is not sufficient to discern the microstructure in the walls. However, SEM micrographs (inset in Fig. 2b) indicate that the sintering stage produced a partially sintered microstructure with porosity of the order of 25% within the walls of these ceramics [10]. Coarsening leads to YSZ and LSM particles with approximately 500 nm and 800 nm sizes, respectively.

Numerical microstructures were generated using the nanotomography images. A mixture of spherical particles of 500 nm and 800 nm diameters, representing YSZ and LSM particles, respectively, were first randomly packed into a cubical simulation box with a 60:40 volume ratio. A total of four million of spheres were necessary to obtain a sufficiently large cube to match the scale of the nanotomography images. The numerical packing was subsequently partially sintered to attain 25% porosity and create solid bonds between particles [13]. The packed particle microstructure was then matched with the 3D nanotomography image by removing particles where the macropores were located (Fig. 2b). Note that although the average particle size and residual porosity were chosen to match the SEM observations of the solid walls, the exact location of each particle cannot be reproduced. Also, partially sintered particles are approximated as spheres indenting each other.

The solid bridges that formed during sintering are modeled as elastic bonds, whose size grows in accordance with Coble's model [14]. Bonds transmit normal and tangential forces as well as resisting moments. The elastic and fracture properties of the dense material that constitute these bonds are summarized in Table 1. In particular, it should be noted that the bond toughness is approximated as $2\,\gamma_s$, thus representing a perfectly brittle material. Bonds may fracture in tension or shear when the stress acting on the bond exceeds the bond strength. A fractured bond does not transmit tensile forces but keeps its compressive stiffness. A Coulomb-like law (friction coefficient: 0.5) is utilized in shear for broken bonds. Force equilibrium is enforced to particles by repositioning each of them using a quasi-static scheme coupled with Newton's second law. A detailed description of the discrete element simulations used here may be found in [13].

The numerical microstructures were uniaxially crushed with lateral free surfaces. Freeze-cast samples exhibit anisotropic microstructures (Fig. 1) that will translate into an anisotropic response [1]. For those anisotropic samples, Fig. 2c shows that three loading directions must be tested. Two may be considered essentially equivalent from a macroscopic point of view (transverse x and y), and will be denominated as transverse. However, it is clear from Fig. 2c that the loading on the transverse x and y directions will lead to significantly different responses at the scale of the small volume tested here.

The stress–strain curves were calculated from the total reaction forces on the crushing planes and from the geometry of the crushed samples. Loading–unloading–reloading cycles were imposed to determine the material stiffness of the numerical samples during the unloading stages. On such porous microstructures, it is questionable that an elastic reversible domain exists. Thus, we prefer the term material stiffness (in units of stress) rather than elastic modulus. The macroscopic strength is also arbitrarily defined as the maximum stress attained during the crushing test (typically attained at $\approx 1\%$ axial strain).

For both the anisotropic and isotropic microstructures considered here, the compressive strength and stiffness have been experimentally

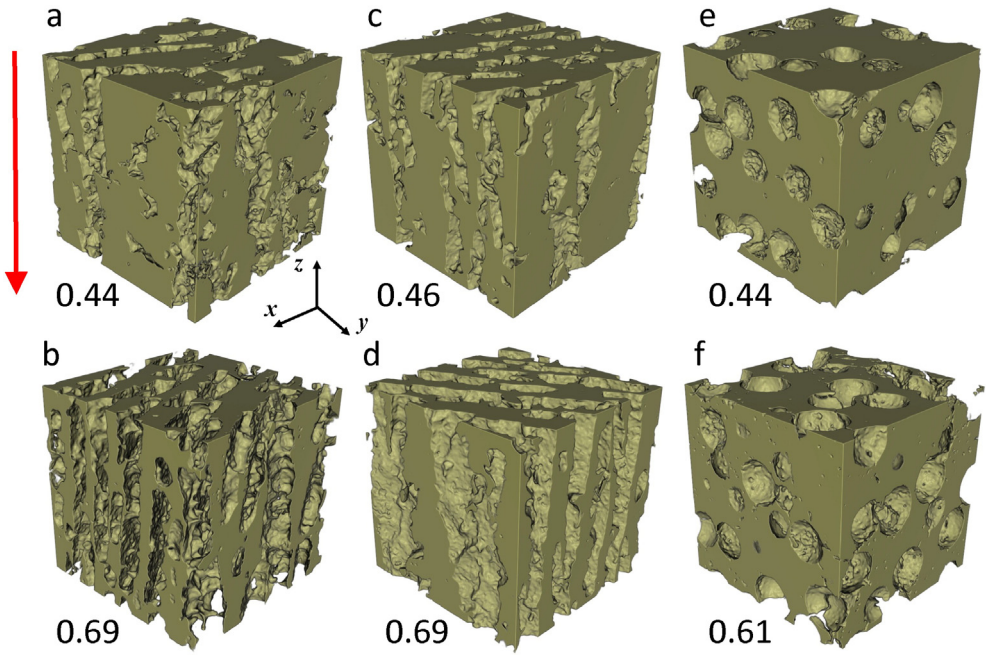

Fig. 1. X-ray nanotomography images. Panels (a–d) correspond to freeze-cast samples (freezing direction indicated by the arrow); panels (e–f) to slip-cast samples. The top row corresponds to low porosity samples (a, c, e) and the bottom row to high porosity samples (b, d, f). The reconstructed volumes are approximately 70^3 to 90^3 μm^3. Numbers indicate the total porosity ε (sum of the wall porosity and of the macroporosity in between walls for freeze-cast samples).